Integrated Sensing Communication Systems in High Mobility Scenarios

Athina Petropulu

Rutgers University

Acknowlegments

Kailong Wang

NSF ECCS-2514270

April 23, 2026

Vision of 6G Wireless Systems

Usage scenarios

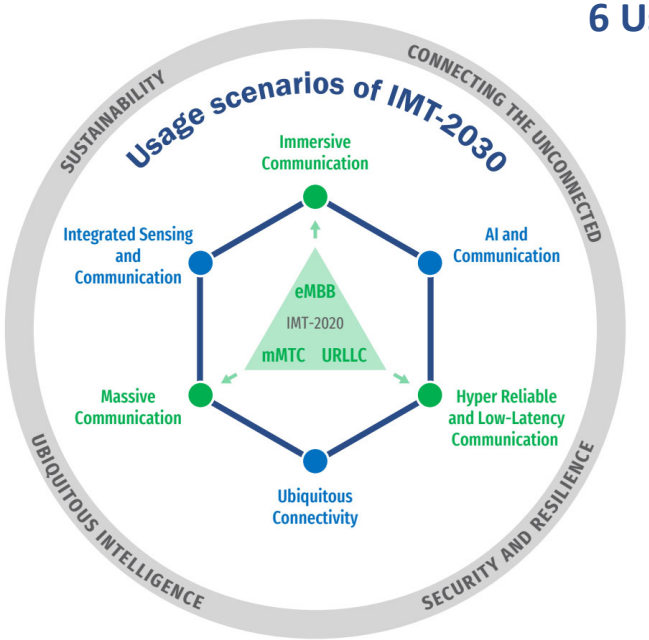

So called "Wheel diagram"
Source: Document 5/131 and edited in SG 5

6 Usage scenarios

Extension from IMT-2020 (5G)

- eMBB ➡ Immersive Communication
- mMTC ➡ Massive Communication
- URLLC ➡ HRLLC (Hyper Reliable & Low-Latency Communication)

New

- Ubiquitous Connectivity
- AI and Communication
- Integrated Sensing and Communication

4 Overarching aspects:

act as design principles commonly applicable to all usage scenarios

Sustainability, Connecting the unconnected,
Ubiquitous intelligence, Security/resilience

Integrated Sensing and Communication (ISAC) Systems

- Communication and radar systems share many commonalities in terms of signal processing algorithms and system architecture.
- In order to access more bandwidth, wireless communication systems have been shifting to higher frequency bands, which were traditionally allocated to radar systems.
- The hardware and frequency convergence has generated a lot of interest in ISAC systems.

Dual Function Radar Communication (DFRC) Systems

- ISAC systems could integrate sensing signals and communication signals on the same platform via time, frequency, code, polarization, or antenna multiplexing.
  - not bandwidth efficient
  - requires complex transmitter hardware
- DFRC systems are ISAC systems that utilize the same waveform for both sensing and communication.
  - high spectral efficiency
  - simple transmitter hardware
  - less expensive device

Dual Function Radar Communication (DFRC) Systems

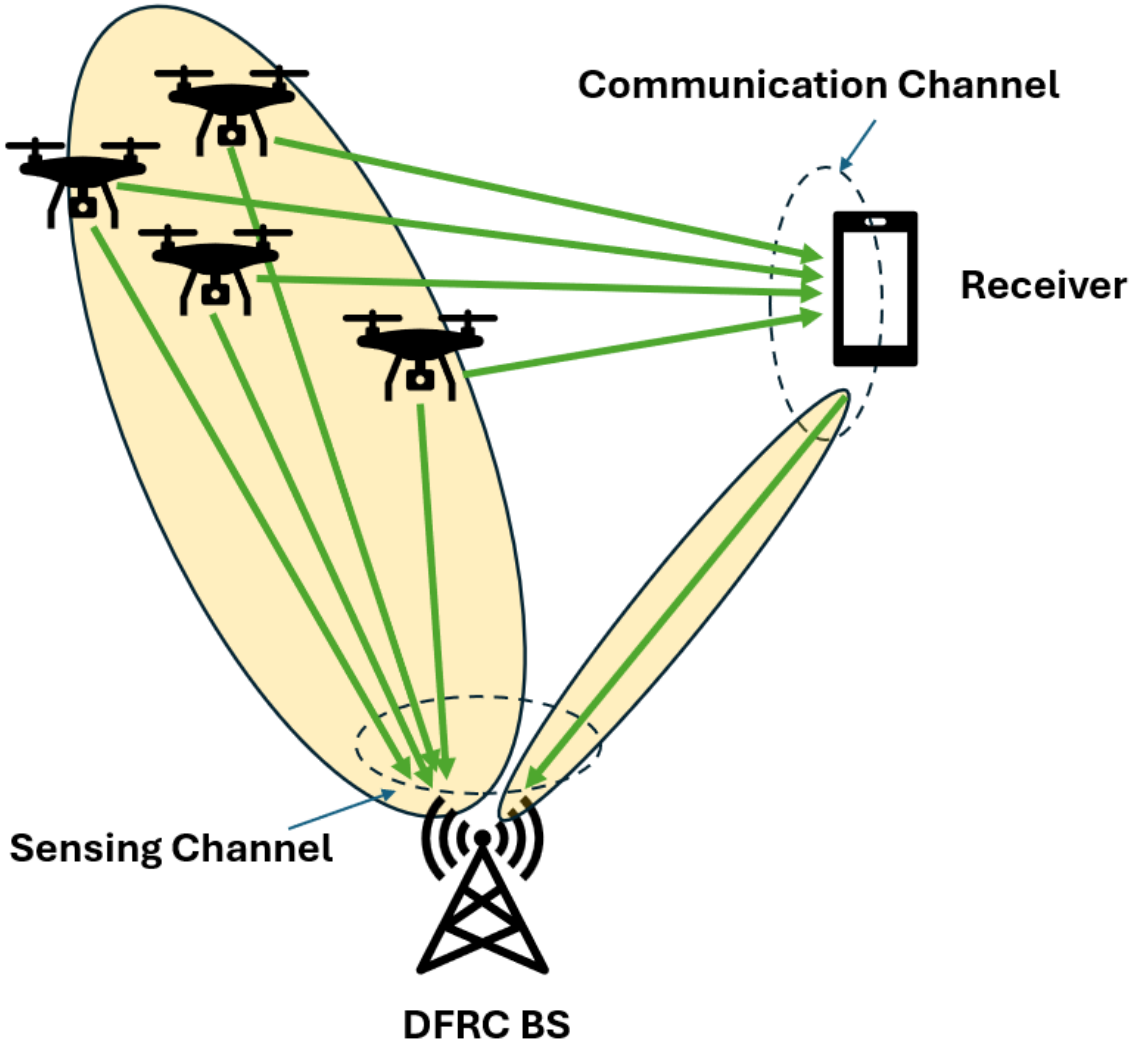

DFRC for Next-Gen Wireless Systems - Requirements and Challenges

- **High Bandwidth for Joint Communication & Sensing**
  - **MIMO for communications**: mature, high-capacity technology
  - **MIMO radar**: flexible beampattern control; virtual aperture for high angular resolution
  - **DFRC trade-offs**: simultaneous MIMO for sensing & communications introduces resource tension
- **High Mobility Support**
  - Fast time-varying channels due to large Doppler shifts
  - More frequent channel estimation & tracking needed
- **Operation at High Frequencies (mmWave/THz)**
  - Enables wide bandwidth $\Rightarrow$ high range resolution
  - Larger Doppler shifts even under moderate motion

- **Possible Solution**: MIMO ISAC using OTFS Waveforms

Orthogonal Time Frequency Space (OTFS) Background

OTFS Waveforms

- OTFS modulation[1] is robust to high Doppler shifts.
- OTFS multiplexes the data symbols in the Doppler-delay (DD) domain.
- A time-varying channel with constant Doppler appears time-invariant in the DD domain.
- For ISAC, OTFS provides a unifying framework for treating sensing and communication.

[1] R. Hadani, S. Rakib, M. Tsatsanis, *et al.*, "Orthogonal Time Frequency Space Modulation", in *2017 IEEE Wireless Communications and Networking Conference (WCNC)*, San Francisco, CA, USA: IEEE, Mar. 2017, pp. 1–6, ISBN: 978-1-5090-4183-1. DOI: 10.1109/WCNC.2017.7925924.

OTFS–Grid Design

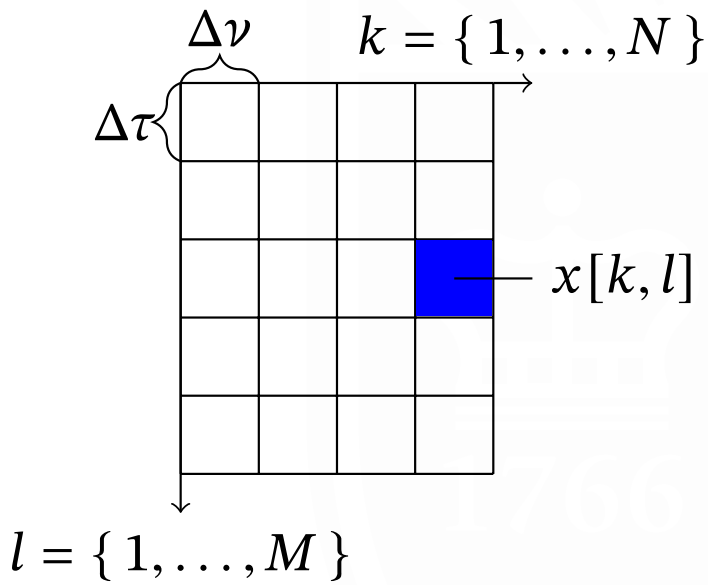

(a) Doppler-delay Grid.

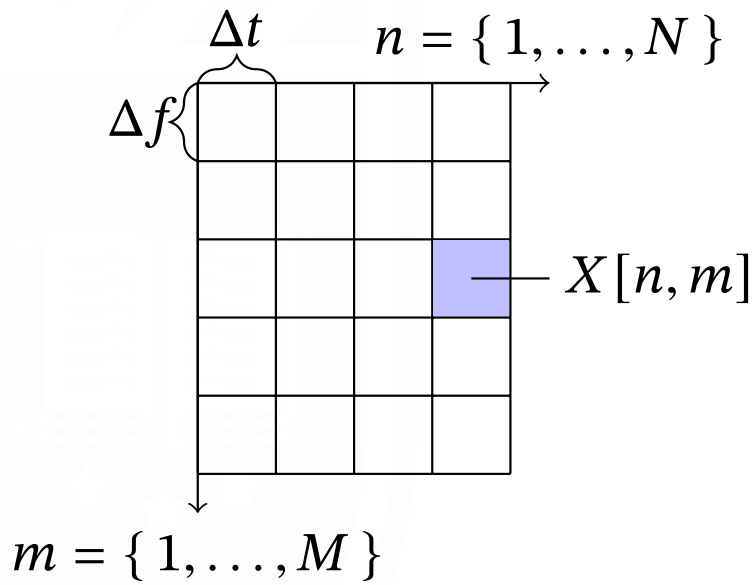

(b) Time-frequency Grid.

- $\Delta\nu = \frac{1}{N\Delta t}$ and $\Delta\tau = \frac{1}{M\Delta f}$
- $\Delta t \cdot \Delta f = 1$: orthogonality in TF domain

OTFS–Modulation

- The symbols are mapped to the TF domain via the Inverse Symplectic Finite Fourier Transform (ISFFT)

$$X[n,m] = \frac{1}{NM} \sum_{k=0}^{N-1} \sum_{l=0}^{M-1} x[k,l] e^{i2\pi\left(\frac{kn}{N} - \frac{ml}{M}\right)}.$$

- The analog signal for transmission, $s(t)$, is created via the Heisenberg Transform

$$s(t) = \sum_{n=0}^{N-1} \sum_{m=0}^{M-1} X[n,m] g_{tx}(t - n\Delta t) e^{i2\pi m\Delta f(t-n\Delta t)}.$$

OTFS–Modulation Visualization

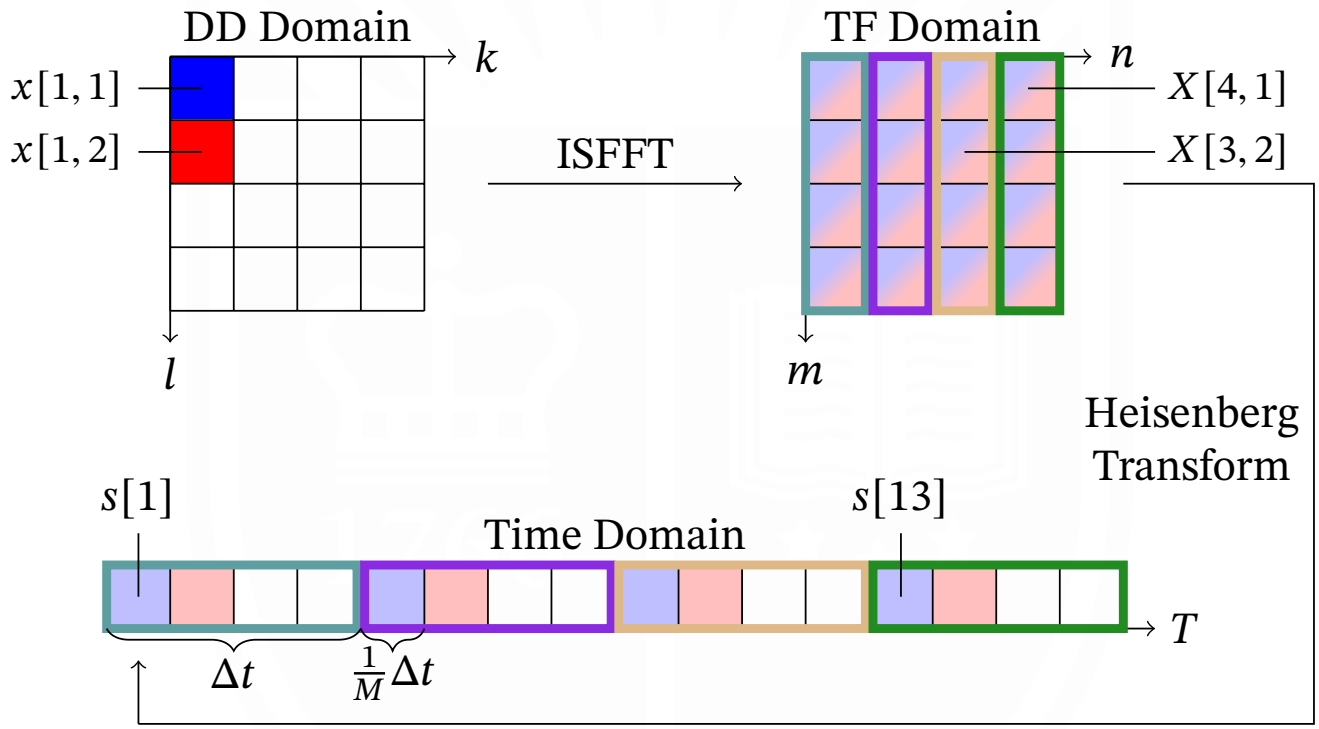

- $T = N\Delta t$: duration of an OTFS symbol $(\Delta\nu = \frac{1}{N\Delta t})$
- $B = M\Delta f$: bandwidth of an OTFS symbol $(\Delta\tau = \frac{1}{M\Delta f})$

DD Domain Sensing/Communication Channel Model

$$h(\nu,\tau)=\sum_{j=0}^{J-1}\beta_j\delta(\nu-\nu_j)\delta(\tau-\tau_j).$$

J/J_T: Number of scatterers/targets.

ν_j: Doppler shift corresponding to Speed v_j

$$\nu_j = 2v_j f/c = (k_j+\kappa_j)\Delta\nu$$
$$k_j\in\mathbb{Z},\quad \kappa_j\in[-0.5,0.5].$$

τ_j: delay corresponding to range R_j

$$\tau_j = 2R_j/c = l_j\Delta\tau$$
$$l_j\in\mathbb{Z}^+.$$

β_j: Complex gain of the j-th target.

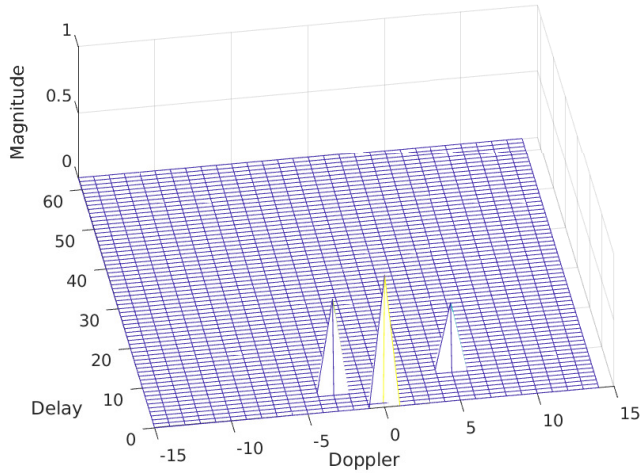

Fig.: A 3-tap channel

I/O for Integer Doppler DD Channel with Ideal Pulses

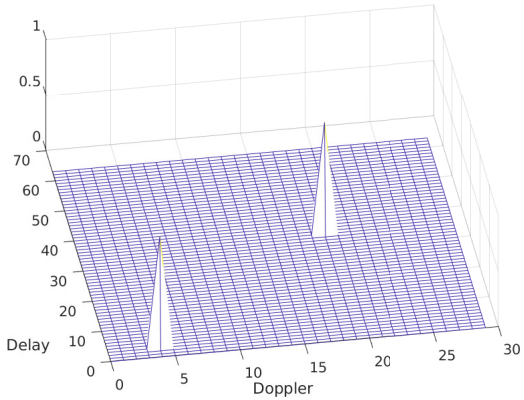

Channel

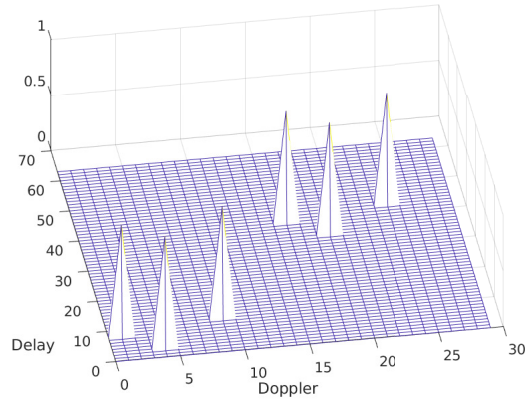

(a) Input with adequate separation

(b) Output contains multiple copies of input

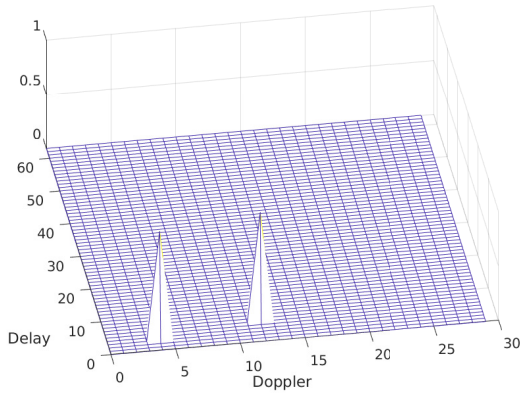

Channel

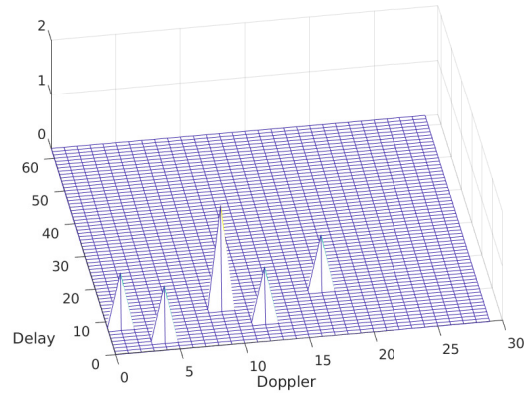

(c) Input without adequate separation

(d) Output has overlapping copies of input

OTFS–Demodulation

- The receiver applies the Wigner Transform of the received signal. Assuming that $g_{tx}(t)$ and $g_{cx}(t)$ are bi-orthogonal it holds that

$$Y[n,m] = X[n,m] \sum_{j=0}^{J-1} H^j[n,m],$$

$$H^j[n,m] = \beta_j e^{-i2\pi\nu_j\tau_j} e^{i2\pi(\nu_j n\Delta t - m\Delta f\tau_j)}.$$

- The demodulated symbols are obtained via SFFT,

$$y[k,l] = \sum_{j=0}^{J-1} \sum_{k'=0}^{N-1} \sum_{l'=0}^{M-1} x[k-k', l-l'] h^j[k',l'],$$

$$h^j[k',l'] = \beta_j e^{-i2\pi \frac{k_j l_j}{NM}} \delta[k'-k_j]_N \delta[l'-l_j]_M,$$

$$\Rightarrow y[k,l] = \sum_{j=0}^{J-1} \beta_j e^{-i2\pi \frac{k_j l_j}{NM}} x[[k-k_j]_N, [l-l_j]_M].$$

In vector form: $\boldsymbol{y} = \boldsymbol{h}\boldsymbol{x} + \boldsymbol{w}$.

Waveform Design and Sensing Channel Estimation

MIMO ISAC With OTFS Waveforms

- MIMO → high communication rate.
  MIMO radar with waveform orthogonality → high spatial resolution via a virtual array.
  MIMO ISAC cannot achieve both.

- Distinct DD bin assignment across antennas[2].

  Good sensing performance but inefficient spectrum utilization.

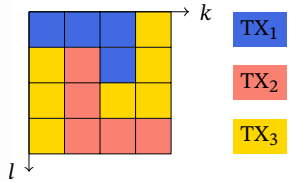

- All DD bins are shared across antennas.

  High communication rate but complex radar detector.

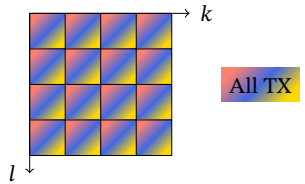

- No prior work can synthesize a VA in a channel with multiple targets.

[2] M. F. Keskin, C. Marcus, O. Eriksson, *et al.*, "Integrated Sensing and Communications With MIMO-OTFS: ISI/ICI Exploitation and Delay-Doppler Multiplexing", *IEEE Transactions on Wireless Communications*, vol. 23, no. 8, pp. 10 229–10 246, Aug. 2024, ISSN: 1536-1276, 1558-2248. DOI: 10.1109/TWC.2024.3370501.

DFRC with Monostatic MIMO Radar Transmitter

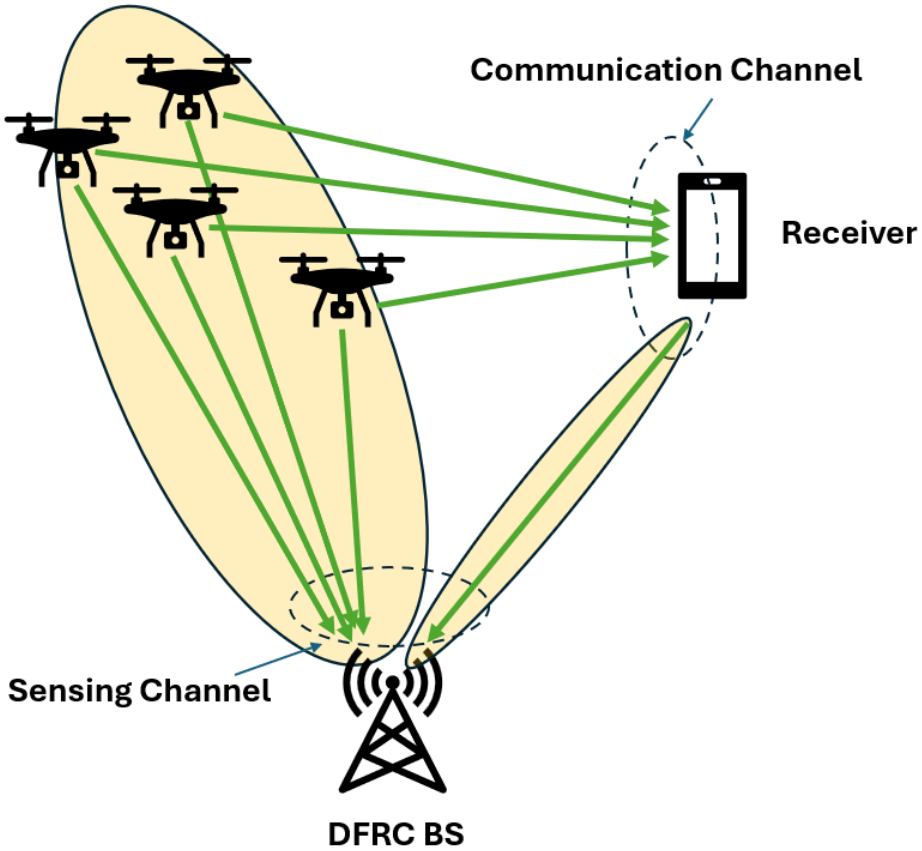

- Transmit waveform design for efficient use of available resources[3]

[3] K. Wang and A. Petropulu, "ISAC MIMO Systems with OTFS Waveforms and Virtual Arrays", *IEEE Journal on Selected Areas in Communications*, pp. 1–1, 2025, ISSN: 1558-0008, 0733-8716. DOI: 10.1109/JSAC.2025.3608761.

OTFS Waveforms with Shared Bins and Ideal Pulses[4]

The transmit and receive antennas form uniform linear arrays with N_t and N_r antennas, respectively, and inter-element spacings g_t and g_r.

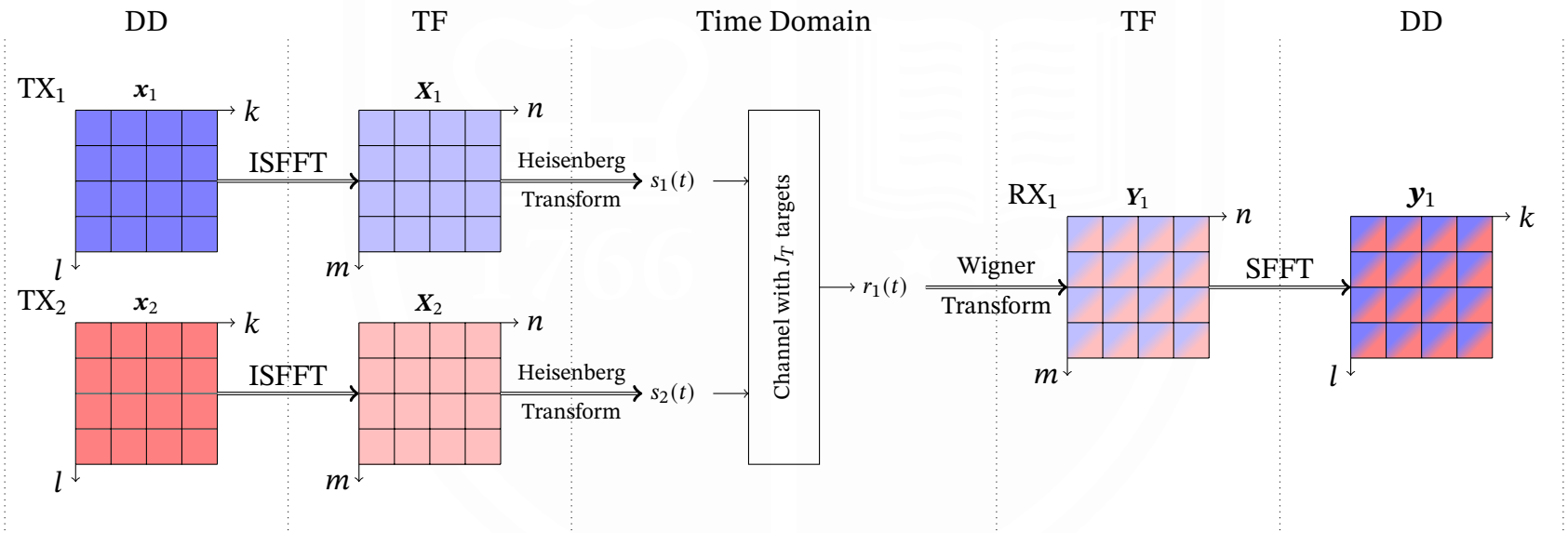

[4] K. Wang and A. Petropulu, "ISAC MIMO Systems with OTFS Waveforms and Virtual Arrays", *IEEE Journal on Selected Areas in Communications*, pp. 1–1, 2025, ISSN: 1558-0008, 0733-8716. DOI: 10.1109/JSAC.2025.3608761.

Coarse Angle Estimation at the Colocated Receiver

- Demodulated symbol of the n_r-th antenna on bin $[k, l]$

$$y_{n_r}[k,l] = \sum_{j=0}^{J_T-1} e^{i2\pi n_r g_r \frac{\sin(\phi_j)}{\lambda}} \sum_{n_t=0}^{N_t-1} e^{-i2\pi n_t g_t \frac{\sin(\phi_j)}{\lambda}} \sum_{k'=0}^{N-1} \sum_{l'=0}^{M-1} x_{n_t}[k-k', l-l'] h_w^j[k', l']$$

$$= \sum_{j=0}^{J_T-1} e^{i2\pi n_r \omega_j} A_j[k,l].$$

$$\omega_j = g_r \frac{\sin(\phi_j)}{\lambda}, \qquad \phi_j = \arcsin\left(\frac{\lambda}{g_r}\omega_j\right).$$

- $\{y_{n_r}[k,l] \mid n_r = 0, 1, \ldots, N_r - 1\}$: sum of J_T complex sinusoids (ω_j).
- Use N_r point DFT to estimate ω_j and then ϕ_j.
- Repeat estimation on various $[k, l]$ to improve the angle estimate.

Coarse Range and Speed Estimation at the Colocated Receiver

- Suppose that there are N_j targets corresponding to angle ϕ_j. Then

$$A_j[k,l] = \sum_{n_t=0}^{N_t-1} e^{-i2\pi n_t g_t \frac{\sin(\phi_j)}{\lambda}} \sum_{j_q=0}^{N_j-1} \sum_{k'=0}^{N-1} \sum_{l'=0}^{M-1} x_{n_t}[k-k', l-l'] h_w^{j_q}[k', l'].$$

$$h_w^{j_q}[k,l] = \beta_{j_q} e^{-i2\pi \frac{k_{j_q} l_{j_q}}{NM}} \delta[k-k_{j_q}]_N \delta[l-l_{j_q}]_M.$$

- Based on known transmitted symbols and estimated angle, define

$$\tilde{A}_j[k,l] \triangleq \sum_{n_t=0}^{N_t-1} e^{-i2\pi n_t g_t \frac{\sin(\phi_j)}{\lambda}} x_{n_t}[k,l].$$

$$A_j[k,l] = \sum_{j_q=0}^{N_j-1} \tilde{A}_j[[k-k_{j_q}]_N, [l-l_{j_q}]_M]$$

- Cross-correlation with $\tilde{A}_j[k,l] \rightarrow (k_{j_q}, l_{j_q}) \xrightarrow{(\Delta\nu,\Delta\tau)} (\nu_{j_q}, \tau_{j_q})$

Limitation of Coarse Estimates

- The resolution of the above-described angle estimates is limited by the receive array.

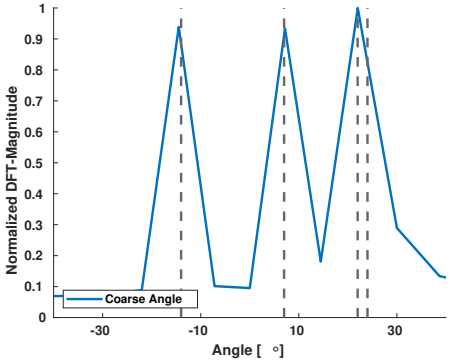

(a) Close targets fall into the same DFT-Angle bin.

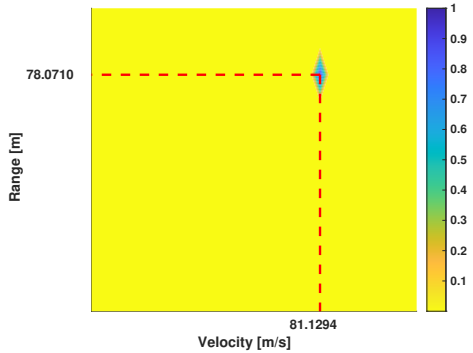

(b) Target in the second angle bin appears as a sharp peak.

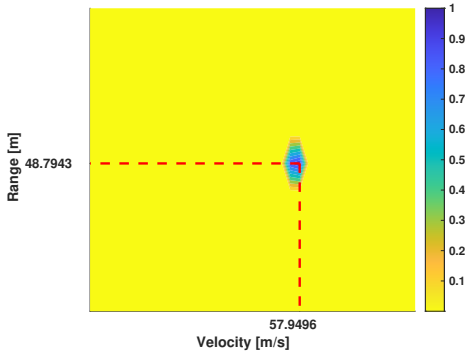

(c) Targets in the third angle bin overlap.

Limitation of Coarse Estimates

- The resolution of the above-described angle estimates is limited by the receive array.
- Next, we show how to construct a virtual array (VA), which will leverage the coarse estimates to provide target estimates beyond the resolution limit of the receive array.
- To achieve this, we modify the transmit waveforms by introducing the concept of private TF domain bins along with some DD domain and TF domain guard bins.
- The introduction of private bins necessitates a slight reduction in the DD-domain information, leading to a trade-off between sensing performance and communication rate.

OTFS Waveforms with Private TF Bins, and TF, DD Guard Bins[5]

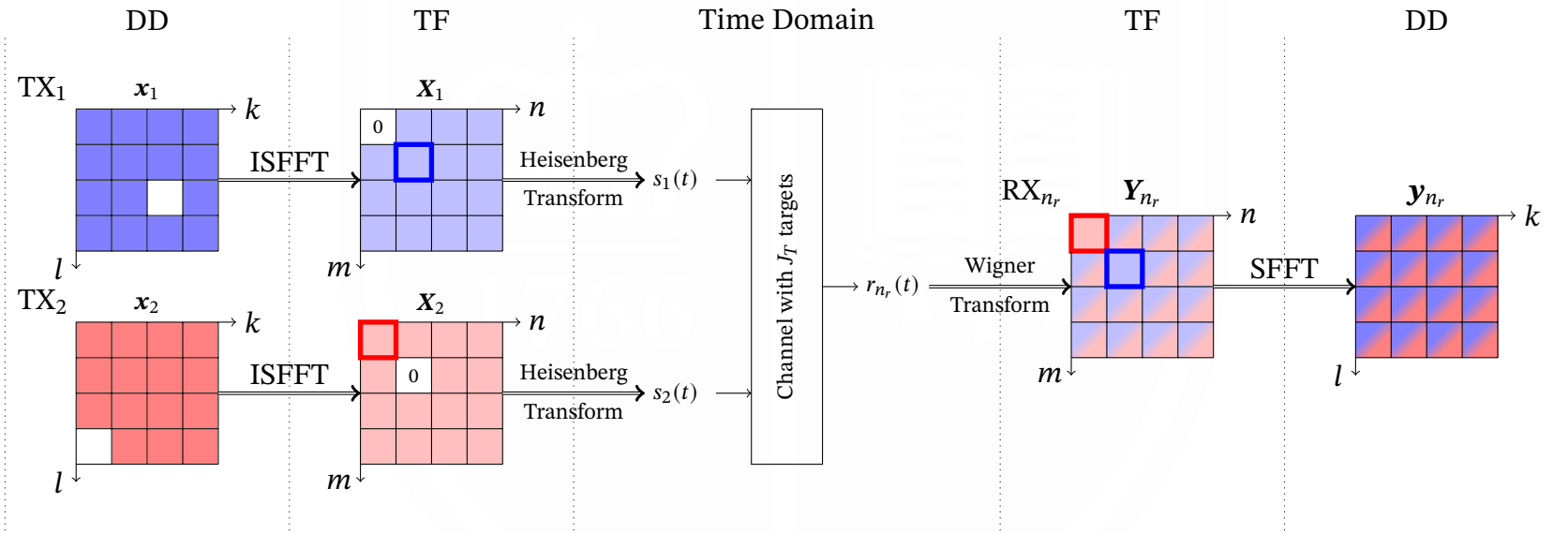

[5] K. Wang and A. Petropulu, "ISAC MIMO Systems with OTFS Waveforms and Virtual Arrays", *IEEE Journal on Selected Areas in Communications*, pp. 1–1, 2025, ISSN: 1558-0008, 0733-8716. DOI: 10.1109/JSAC.2025.3608761.

TF Domain–Shared *vs.* Private Bins

- Shared bin

$$Y_{n_r}[n,m] = \sum_{j=0}^{J_T-1} \sum_{n_t=0}^{N_t-1} e^{i2\pi(n_r g_r - n_t g_t)\frac{\sin(\phi_j)}{\lambda}} X_{n_t}[n,m] H^j[n,m].$$

- Private bin

$$Y_{n_r}[n_p,m_p] = X_p[n_p,m_p] \sum_{j=0}^{J_T-1} e^{i2\pi(n_r g_r - p g_t)\frac{\sin(\phi_j)}{\lambda}} H^j[n_p,m_p].$$

$$H^j[n,m] = \beta_j e^{-i2\pi\frac{k_j l_j}{NM}} e^{\left(\frac{k_j n}{N} - \frac{m l_j}{M}\right)}.$$

Virtual Array (VA) and Sparse Signal Recovery (SSR)

- Place the ratio $Y_{n_r}[n_p, m_p]/X_p[n_p, m_p]$ of all receive antennas in $\boldsymbol{r}_p$,

$$\boldsymbol{r}_p = \sum_{j=0}^{J_T-1} \beta_j \boldsymbol{\Phi}_p(\phi_j, \nu_j, \tau_j; n_p, m_p) = \boldsymbol{\Phi}_p \boldsymbol{\beta}.$$

- The (n_r, j)-th element of $\boldsymbol{\Phi}_p$ is

$$e^{i2\pi(n_r g_r - p g_t)\frac{sin(\phi_j)}{\lambda}} e^{-i2\pi \frac{k_j l_j}{NM}} e^{i2\pi\left(\frac{k_j n_p}{N} - \frac{m_p l_j}{M}\right)}.$$

- Stack all N_p vectors $\boldsymbol{r}_p$ in vector $\boldsymbol{r} \in \mathbb{C}^{N_p N_r}$ to get

$$\boldsymbol{r} = \boldsymbol{\Phi}\boldsymbol{\beta} \quad \text{(virtual array)}$$

- Express $\boldsymbol{r}$ in terms of an overcomplete basis $\tilde{\boldsymbol{\Phi}}$, constructed based on a discretization of the target space around the coarse estimates. Then, $\tilde{\boldsymbol{\beta}}$ is a sparse vector, indicating the presence of a target on grid points.
- Use sparse signal recovery (SSR) methods to obtain $\tilde{\boldsymbol{\beta}}$.

Communication-Sensing Performance Trade-Off

- Zero-forcing of TF bins requires reducing DD-domain information symbols → communication–sensing trade-off.
- Using N_p private bins yields an N_p-fold improvement in sensing performance, while reducing the total number of information bearing symbols by

$$\eta = \frac{N_p(N_t - 1)}{N_t NM}.$$

- Even a small N_p provides substantial sensing gains, leading to only a minor reduction in communication rate.
  ($N_p = N_t = 4, M = 128, N = 64 \rightarrow \eta = 0.037\%$)

Integer Doppler DD Channel with Rectangular Pulses

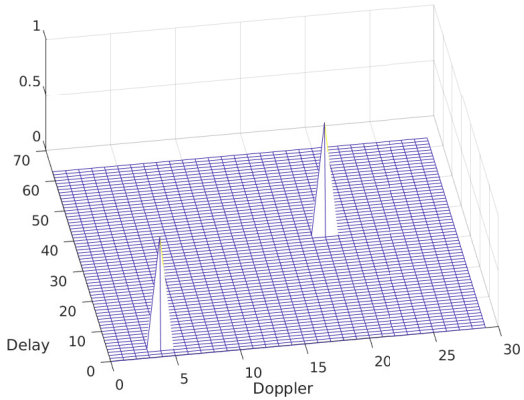

Channel

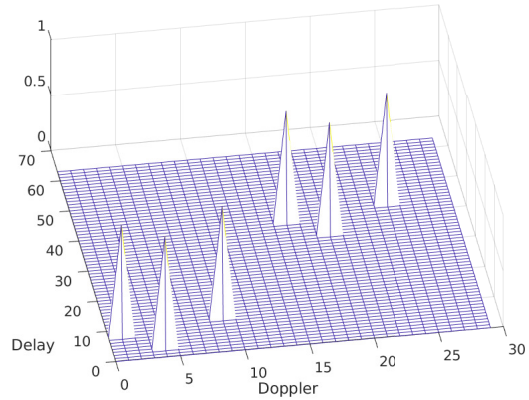

(a) Input with adequate separation

(b) Output contains multiple copies of input

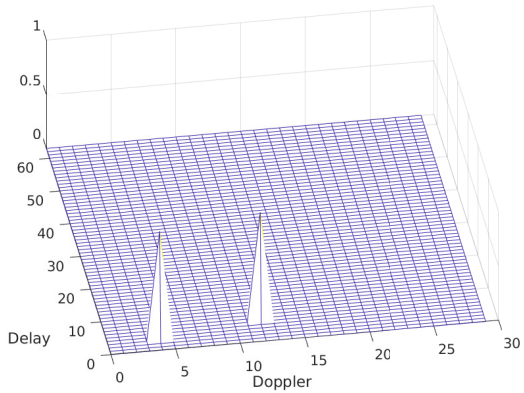

Channel

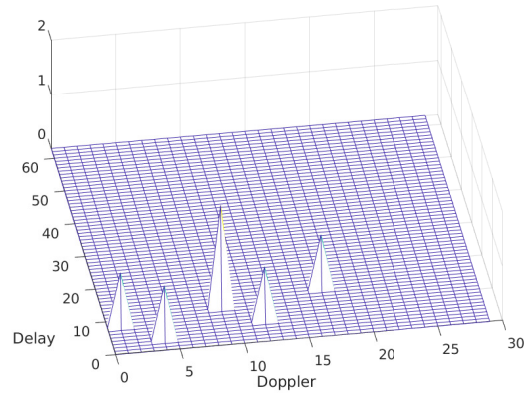

(c) Input without adequate separation

(d) Output has overlapping copies of input

MIMO-OTFS DD I/O with Rectangular Pulses

- Assuming the use of a cyclic prefix (CP) that avoids interference between OTFS symbols, the DD channel I/O becomes

$$\tilde{y}_{n_r}[k,l] = \sum_{j=0}^{J_T-1} \sum_{n_t=0}^{N_t-1} e^{i2\pi(n_r g_r - n_t g_t)\frac{\sin(\phi_j)}{\lambda}} \beta_j e^{-i2\pi\frac{k_j l_j}{NM}} \times \alpha_j[k,l] x_{n_t}[[k-k_j]_N, [l-l_j]_M],$$

$$\alpha_j[k,l] = \begin{cases} e^{i2\pi\frac{k_j l}{NM}} & l_j \le l < M, \\ \frac{N-1}{N} e^{i2\pi\frac{k_j l}{NM}} e^{-i2\pi\frac{[k-k_j]_N}{N}} & 0 \le l < l_j. \end{cases}$$

- Coarse angle estimate, range and speed estimation can still be obtained as described above. The virtual array construction will be different.

MIMO-OTFS TF I/O with Rectangular Pulses[6]

$$\tilde{Y}_{n_r}[n,m] = \sum_{n_t=0}^{N_t-1} X_{n_t}[n,m] \sum_{j=0}^{J_T-1} e^{i2\pi(n_r g_r - n_t g_t)\frac{\sin(\phi_j)}{\lambda}} \beta_j e^{-i2\pi\frac{k_j l_j}{NM}}$$

$$\times e^{i2\pi\left(\frac{k_j n}{N} - \frac{m l_j}{M}\right)} \xi_j + \tilde{I}_{n_r}[n,m] \qquad \text{(Treat } \tilde{I}_{n_r}[n,m] \text{ as zero-mean noise)}$$

$$\tilde{I}_{n_r}[n,m] = \sum_{n_t=0}^{N_t-1} \sum_{m'\neq m} \sum_{n'\neq n} X_{n_t}[n',m'] \sum_{j=0}^{J_T-1} e^{i2\pi(n_r g_r - n_t g_t)\frac{\sin(\phi_j)}{\lambda}} \beta_j e^{-i2\pi\frac{k_j l_j}{NM}}$$

$$\times \frac{1}{NM} \sum_{k=0}^{N-1} \sum_{l=0}^{M-1} \alpha_j[k,l] e^{-i2\pi\left(\frac{k(n'-n)-k_j n'}{N} - \frac{(m'-m)l - m' l_j}{M}\right)}$$

$$\xi_j = \frac{1}{NM} \sum_{k=0}^{N-1} \sum_{l=0}^{M-1} \alpha_j[k,l] = \frac{1}{M} \frac{e^{i2\pi\frac{k_j l_j}{NM}} - e^{i2\pi\frac{k_j}{N}}}{1 - e^{i2\pi\frac{k_j}{NM}}}$$

[6] K. Wang and A. Petropulu, "ISAC MIMO Systems with OTFS Waveforms and Virtual Arrays", *IEEE Journal on Selected Areas in Communications*, pp. 1–1, 2025, ISSN: 1558-0008, 0733-8716. DOI: 10.1109/JSAC.2025.3608761.

Virtual Array with Rectangular Pulses

- Evaluate the received TF domain signal on private bins

$$\tilde{Y}_{n_r}[n_p, m_p] = X_p[n_p, m_p] \sum_{j=0}^{J_T-1} e^{i2\pi(n_r g_r - p g_t)\frac{sin(\phi_j)}{\lambda}} \beta_j e^{-i2\pi \frac{k_j l_j}{NM}} \times e^{i2\pi\left(\frac{k_j n_p}{N} - \frac{m_p l_j}{M}\right)} \xi_j + \tilde{I}_{n_r}[n_p, m_p].$$

- Place the ratio $\tilde{Y}_{n_r}[n_p, m_p]/X_p[n_p, m_p]$ of all receive antennas to get

$$\boldsymbol{r}_p = \boldsymbol{\Phi}_p \boldsymbol{\beta}.$$

- The (n_r, j)-th element of $\boldsymbol{\Phi}_p$ is

$$e^{i2\pi(n_r g_r - p g_t)\frac{sin(\phi_j)}{\lambda}} e^{-i2\pi \frac{k_j l_j}{NM}} e^{i2\pi\left(\frac{k_j n_p}{N} - \frac{m_p l_j}{M}\right)} \xi_j.$$

- The virtual array can be constructed by stacking all N_p vectors $\boldsymbol{r}_p$.

Fractional Doppler DD Channel with Rectangular Pulses

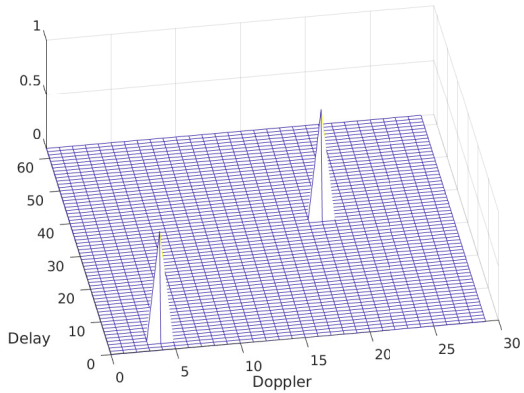

Channel

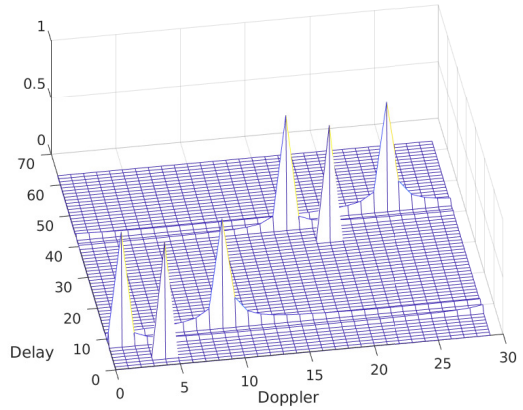

(a) Input with adequate separation

(b) Output contains multiple copies of input and observable power leakage

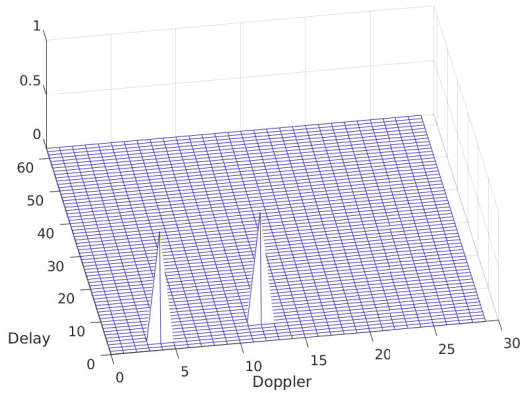

Channel

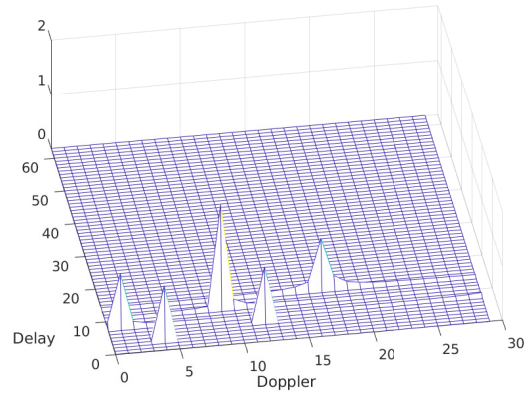

(c) Input without adequate separation

(d) Output has overlapping copies of input and observable power leakage

MIMO-OTFS with Rectangular Pulses and Fractional Doppler[7,8]

- Received DD domain signal

$$\tilde{y}_{n_r}[k,l] = \sum_{j=0}^{J_T-1} \sum_{n_t=0}^{N_t-1} e^{i2\pi(n_r g_r - n_t g_t)\frac{\sin(\phi_j)}{\lambda}} \beta_j e^{-i2\pi\frac{(k_j+\kappa_j)l_j}{NM}}$$

$$\times \sum_{q=k_j-(N-1)}^{k_j} \alpha_j[k,l,q]\, x_{n_t}[[k-(k_j-q)]_N, [l-l_j]_M],$$

$$\alpha_j[k,l,q] = \begin{cases} \frac{1}{N}\gamma_j(q) e^{i2\pi\frac{(k_j+\kappa_j)l}{NM}} & l_j \le l < M \\ \frac{1}{N}(\gamma_j(q)-1) e^{i2\pi\frac{(k_j+\kappa_j)l}{NM}} e^{-i2\pi\frac{[k-(k_j-q)]_N}{N}} & 0 \le l < l_j \end{cases}$$

with $\gamma_j(q) = \frac{e^{-i2\pi(-q-\kappa_j)}-1}{e^{-i2\pi(-q-\kappa_j)/N}-1} \neq N$ due to the fractional term κ_j.

[7] K. Wang and A. Petropulu, "ISAC MIMO Systems with OTFS Waveforms and Virtual Arrays", *IEEE Journal on Selected Areas in Communications*, pp. 1–1, 2025, ISSN: 1558-0008, 0733-8716. DOI: 10.1109/JSAC.2025.3608761.

[8] K. Wang and A. Petropulu, *Low overhead and scalable time-frequency pilots design for mimo otfs channel estimation*, 2026. arXiv: 2511.08504 [eess.SP]. [Online]. Available: https://arxiv.org/abs/2511.08504.

MIMO-OTFS with Rectangular Pulses and Fractional Doppler[7,8]

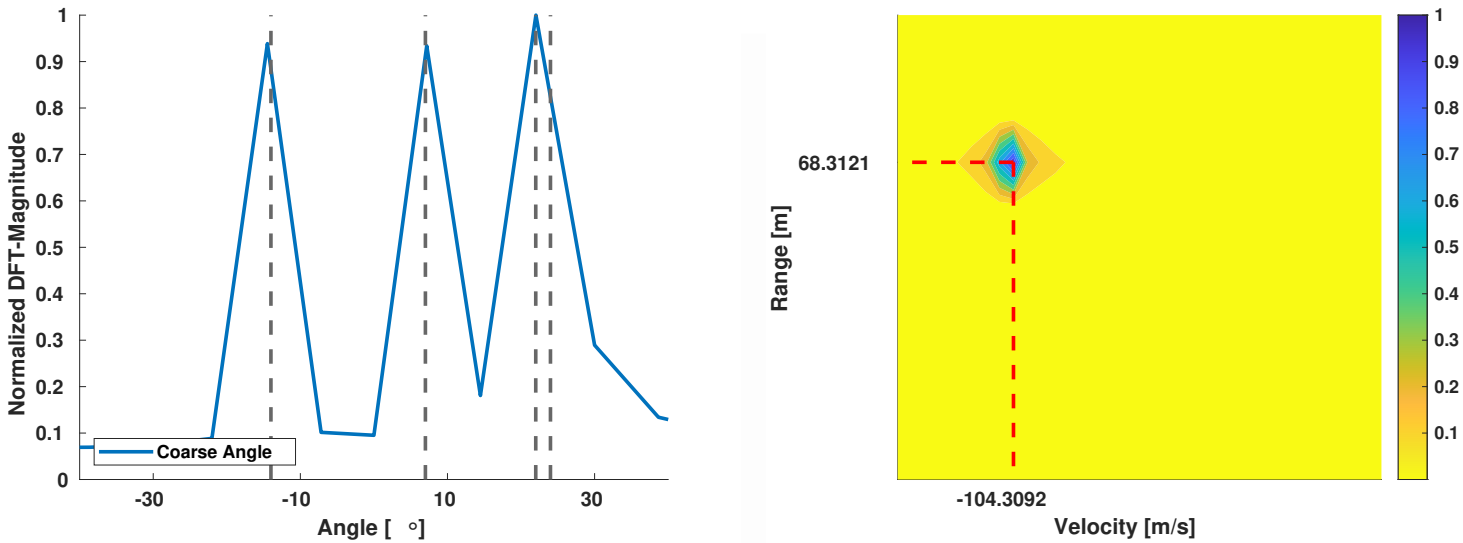

Fig.: Single target in the first angle bin shows a wide peak after cross-correlation.

[7] K. Wang and A. Petropulu, "ISAC MIMO Systems with OTFS Waveforms and Virtual Arrays", *IEEE Journal on Selected Areas in Communications*, pp. 1–1, 2025, ISSN: 1558-0008, 0733-8716. DOI: 10.1109/JSAC.2025.3608761.

[8] K. Wang and A. Petropulu, *Low overhead and scalable time-frequency pilots design for mimo otfs channel estimation*, 2026. arXiv: 2511.08504 [eess.SP]. [Online]. Available: https://arxiv.org/abs/2511.08504.

MIMO-OTFS with Rectangular Pulses and Fractional Doppler[7,8]

- The n_r-th antenna received TF signal on the private bin is

$$\tilde{Y}_{n_r}[n_p, m_p] = X_p[n_p, m_p] \sum_{j=0}^{J_T-1} e^{i2\pi(n_r g_r - p g_t)\frac{\sin(\phi_j)}{\lambda}} \beta_j e^{-i2\pi\frac{(k_j+\kappa_j)l_j}{NM}} \times e^{i2\pi\left(\frac{(k_j+\kappa_j)n_p}{N} - \frac{m_p l_j}{M}\right)} \xi_j + \tilde{I}_{n_r}[n_p, m_p],$$

where

$$\xi_j = \frac{1}{M} \frac{e^{i2\pi\frac{(k_j+\kappa_j)l_j}{NM}} - e^{i2\pi\frac{(k_j+\kappa_j)}{N}}}{1 - e^{i2\pi\frac{(k_j+\kappa_j)}{NM}}}$$

[7] K. Wang and A. Petropulu, "ISAC MIMO Systems with OTFS Waveforms and Virtual Arrays", *IEEE Journal on Selected Areas in Communications*, pp. 1–1, 2025, ISSN: 1558-0008, 0733-8716. DOI: 10.1109/JSAC.2025.3608761.

[8] K. Wang and A. Petropulu, *Low overhead and scalable time-frequency pilots design for mimo otfs channel estimation*, 2026. arXiv: 2511.08504 [eess.SP]. [Online]. Available: https://arxiv.org/abs/2511.08504.

MIMO-OTFS with Rectangular Pulses and Fractional Doppler[7,8]

- Place the ratio $\tilde{Y}_{n_r}[n_p, m_p]/X_p[n_p, m_p]$ of all receive antennas to get

$$\boldsymbol{r}_p = \boldsymbol{\Phi}_p \boldsymbol{\beta}.$$

- The (n_r, j)-th element of $\boldsymbol{\Phi}_p$ is

$$e^{i2\pi(n_r g_r - p g_t)\frac{sin(\phi_j)}{\lambda}} e^{-i2\pi\frac{(k_j+\kappa_j)l_j}{NM}} e^{i2\pi\left(\frac{(k_j+\kappa_j)n_p}{N} - \frac{m_p l_j}{M}\right)\xi_j}.$$

- The virtual array can be constructed by stacking all N_p vectors $\boldsymbol{r}_p$.
- The presence of $\kappa_j \in [-0.5, 0.5]$ requires discretization of the range $[-0.5 : 0.1 : 0.5]$.

[7] K. Wang and A. Petropulu, "ISAC MIMO Systems with OTFS Waveforms and Virtual Arrays", *IEEE Journal on Selected Areas in Communications*, pp. 1–1, 2025, ISSN: 1558-0008, 0733-8716. DOI: 10.1109/JSAC.2025.3608761.

[8] K. Wang and A. Petropulu, *Low overhead and scalable time-frequency pilots design for mimo otfs channel estimation*, 2026. arXiv: 2511.08504 [eess.SP]. [Online]. Available: https://arxiv.org/abs/2511.08504.

Simulations - System and Channel Setup

Symbol	Parameter	Value
M	Number of subcarriers	128
N	Number of subsymbols	64
Δf	Subcarrier spacing	120 KHz
f_c	Carrier frequency	24.25 GHz
g_t	Transmit antenna spacing	0.5λ
g_r	Receive antenna spacing	0.5λ
J_T/J	Number of targets/paths	3
ϕ_j	Angle of targets/paths	$[-14, 7, 22]^\circ$
R_j	Range of targets/paths	$[68.31, 78.07, 48.79]$m
v_j	Speed of targets/paths	$[-104.31, 81.13, 57.95]$m/s

Coarse Estimation Performance

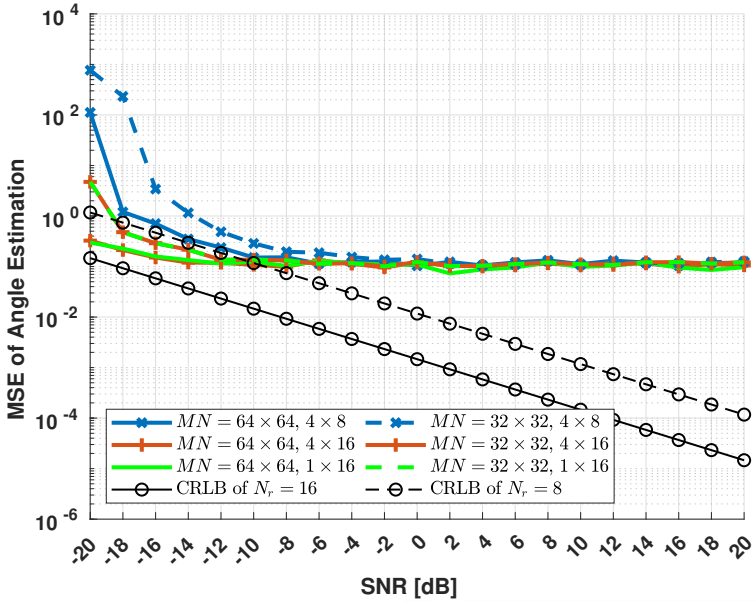

(a) Angle

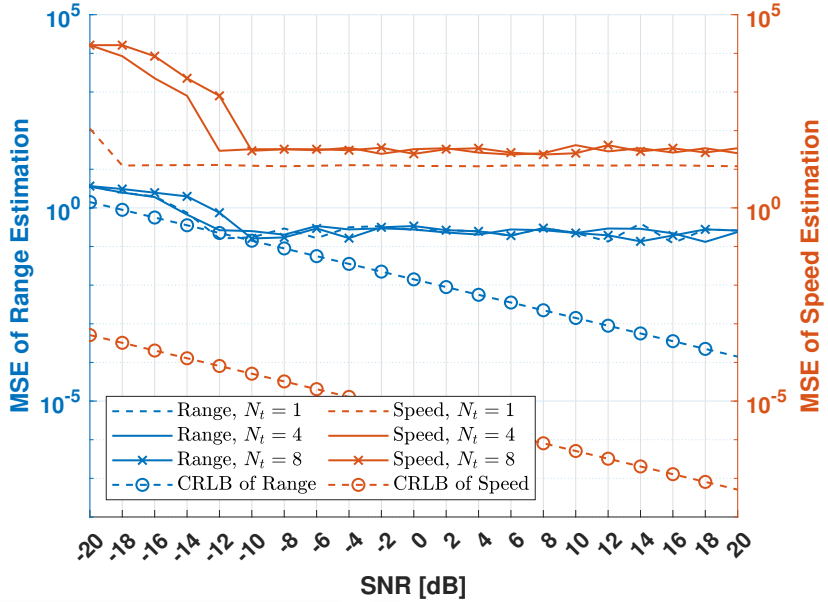

(b) Range and Speed

SSR Speed Estimation with Fractional Doppler

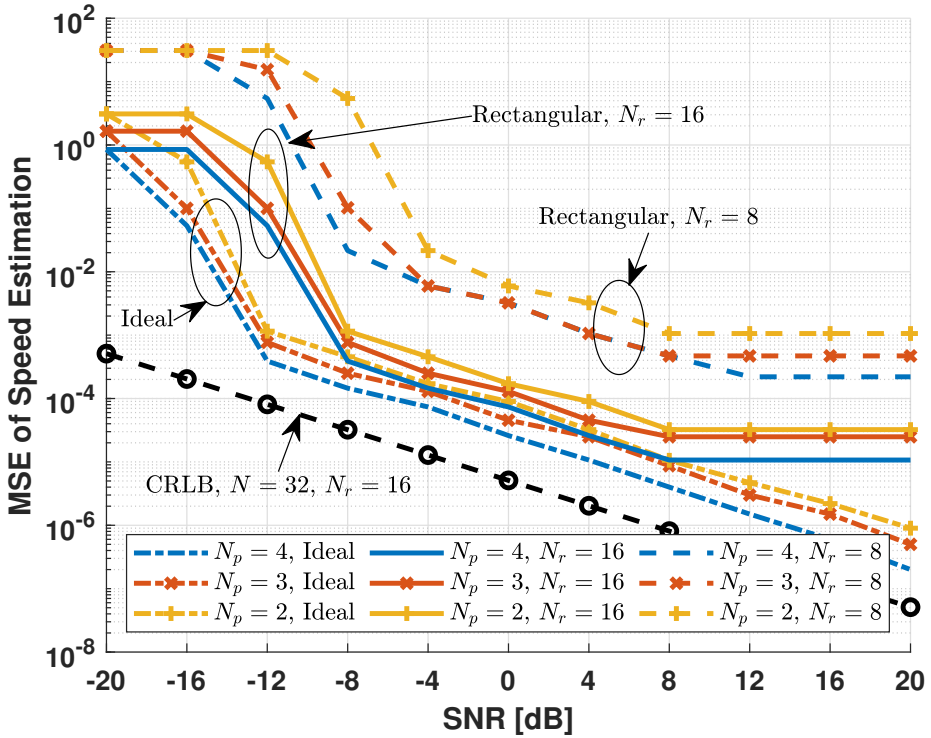

Fig.: SSR Fractional Doppler Estimation (Ideal pulses *vs*. Rectangular pulses).

Waveform Design and Communication Channel Estimation

Existing Works on MIMO OTFS Channel Estimation

- One DD pilot per antenna with non-overlapping guard regions[9]
  - High pilot overhead; does not scale with the number of transmit antennas
- Multiple uncorrelated DD pilots with overlapping guard regions[10]
  - Still results in substantial pilot overhead
- Superimposed DD pilots[11]
  - Requires high-complexity processing to suppress pilot–data interference
  - Accurate estimation requires multiple OTFS frames
- Pilots inserted between OTFS frames[12]
  - Cannot provide in-burst channel estimation

[9] M. Kollengode Ramachandran and A. Chockalingam, "MIMO-OTFS in High-Doppler Fading Channels: Signal Detection and Channel Estimation", in *2018 IEEE Global Communications Conference (GLOBECOM)*, Abu Dhabi, United Arab Emirates: IEEE, Dec. 2018, pp. 206–212, ISBN: 978-1-5386-4727-1. DOI: 10.1109/GLOCOM.2018.8647394.

[10] W. Shen, L. Dai, J. An, *et al.*, "Channel Estimation for Orthogonal Time Frequency Space (OTFS) Massive MIMO", *IEEE Transactions on Signal Processing*, vol. 67, no. 16, pp. 4204–4217, Aug. 2019, ISSN: 1053-587X, 1941-0476. DOI: 10.1109/TSP.2019.2919411.

[11] A. Mehrotra, S. Srivastava, A. K. Jagannatham, *et al.*, "Data-aided csi estimation using affine-precoded superimposed pilots in orthogonal time frequency space modulated mimo systems", *IEEE Transactions on Communications*, vol. 71, no. 8, pp. 4482–4498, 2023. DOI: 10.1109/TCOMM.2023.3280550.

[12] A. Mehrotra, S. Srivastava, S. Asifa, *et al.*, "Online Bayesian Learning-Aided Sparse CSI Estimation in OTFS Modulated MIMO Systems for Ultra-High-Doppler Scenarios", *IEEE Transactions on Communications*, vol. 72, no. 4, pp. 2182–2200, Apr. 2024, ISSN: 0090-6778, 1558-0857. DOI: 10.1109/TCOMM.2023.3342230.

Bistatic Scenario

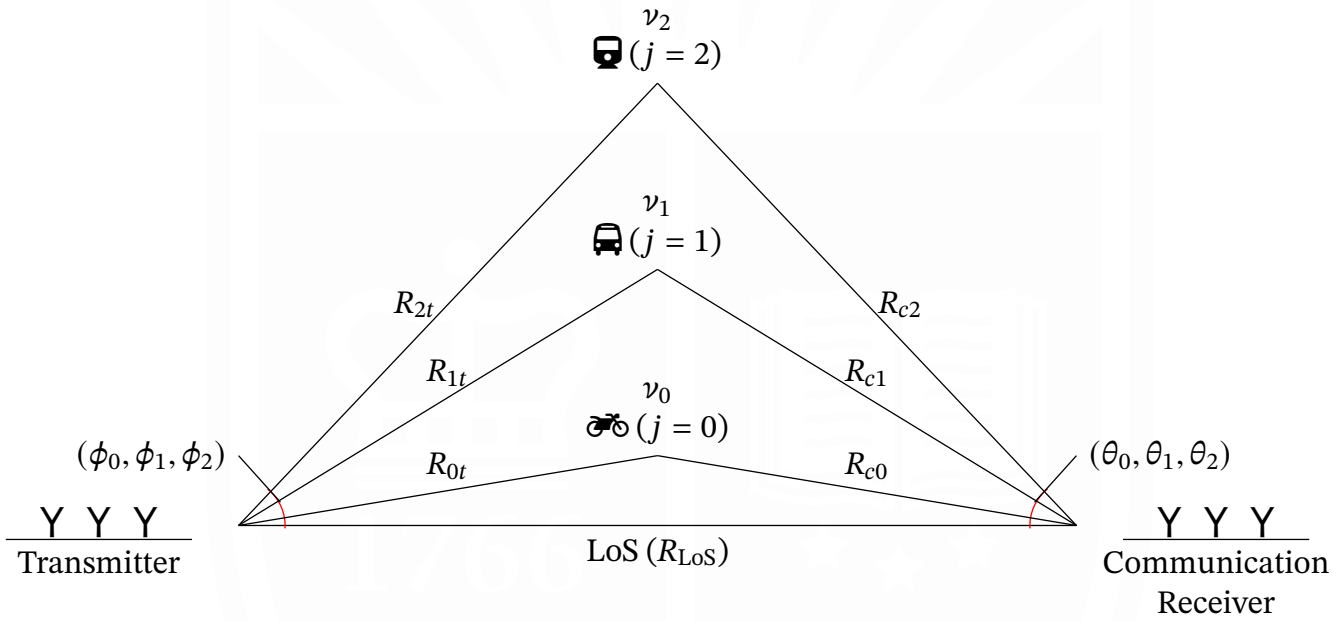

- The communication channel consists of J scatterers, each with parameters $\{\beta_j, \theta_j, \phi_j, \tau_j, \nu_j\}$
- Channel estimation at the communication receiver breaks down to estimating these parameters at the communication receiver.

TF Pilot with TF and DD Guard Bins[13,14]

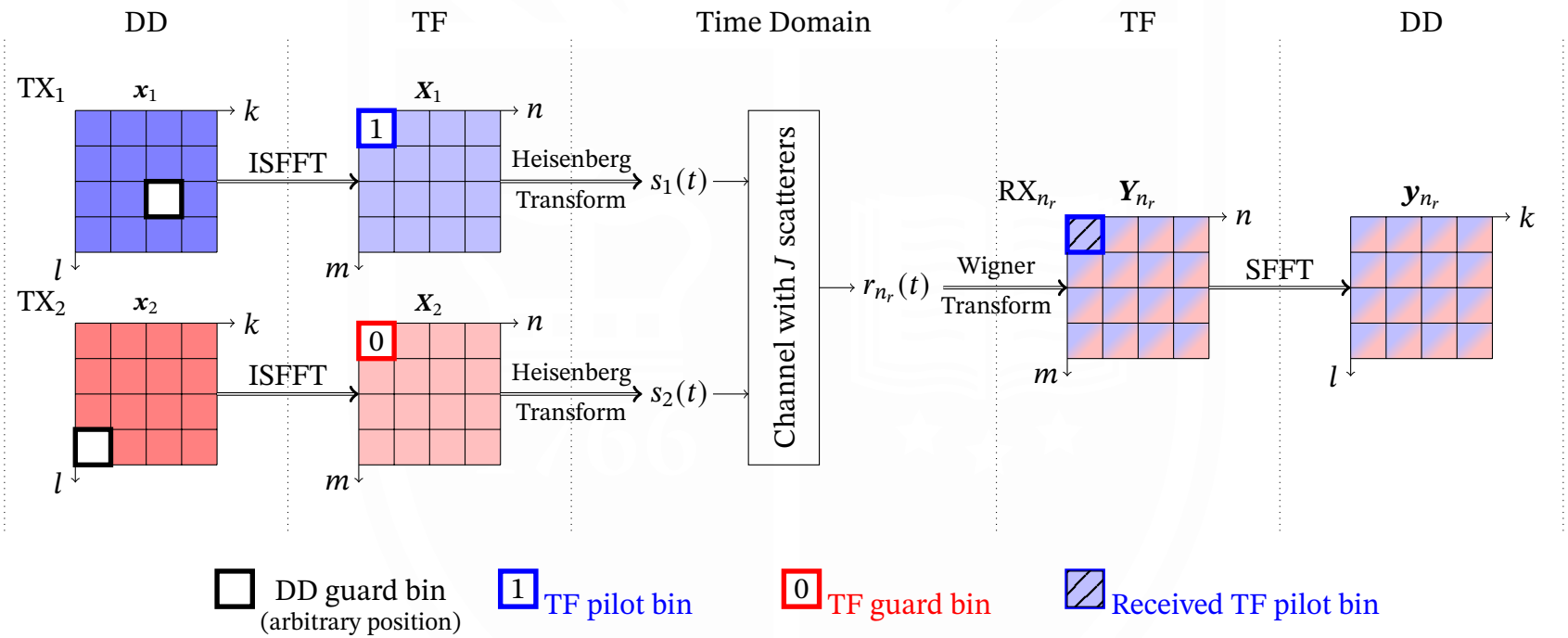

[13] K. Wang and A. Petropulu, "ISAC MIMO Systems with OTFS Waveforms and Virtual Arrays", *IEEE Journal on Selected Areas in Communications*, pp. 1–1, 2025, ISSN: 1558-0008, 0733-8716. DOI: 10.1109/JSAC.2025.3608761.

[14] K. Wang and A. Petropulu, "Low Overhead MIMO-OTFS Channel Estimation", Accepted by The 33rd European Signal Processing Conference (EUSIPCO 2025).

TF Domain *Shared vs. Private* Bins at the Comm. Receiver

- **On a shared bin:**

$$Y_{n_c}[n,m] = \sum_{n_t=0}^{N_t-1} X_{n_t}[n,m] \sum_{j=0}^{J-1} e^{-i2\pi n_c g_c \frac{\sin(\theta_j)}{\lambda}} e^{-i2\pi n_t g_t \frac{\sin(\phi_j)}{\lambda}}$$
$$\times \beta_j e^{-i2\pi \frac{(k_j+\kappa_j)l_j}{NM}} e^{i2\pi\left(\frac{(k_j+\kappa_j)n}{N} - \frac{ml_j}{M}\right)} \xi_j + I_{n_c}[n,m].$$

- **On a private bin:**

$$Y_{n_c}[n_p,m_p] = X_p[n_p,m_p] \sum_{j=0}^{J-1} e^{-i2\pi n_c g_c \frac{\sin(\theta_j)}{\lambda}} e^{-i2\pi p g_t \frac{\sin(\phi_j)}{\lambda}}$$
$$\times \beta_j e^{-i2\pi \frac{(k_j+\kappa_j)l_j}{NM}} e^{i2\pi\left(\frac{(k_j+\kappa_j)n_p}{N} - \frac{m_p l_j}{M}\right)} \xi_j + I_{n_c}[n_p,m_p].$$

Coarse Estimation of Angle of Arrival (AoA) θ_j

Ignoring $I_{n_c}[n,m]$, we can rewrite $Y_{n_c}[n,m]$ as

$$Y_{n_c}[n,m] = \sum_{j=0}^{J-1} A_j[n,m] e^{-i2\pi n_c g_c \frac{\sin(\theta_j)}{\lambda}},$$

$$A_j[n,m] = \sum_{n_t=0}^{N_t-1} X_{n_t}[n,m] e^{-i2\pi n_t g_t \frac{\sin(\phi_j)}{\lambda}} H^j[n,m],$$

$$H^j[n,m] = \beta_j e^{-i2\pi \frac{(k_j+\kappa_j)l_j}{NM}} e^{i2\pi\left(\frac{(k_j+\kappa_j)n}{N} - \frac{ml_j}{M}\right)\xi_j}.$$

- $\{Y_{n_c}[n,m] \mid n_c = 0, 1, \ldots, N_c - 1\}$: sum of J complex sinusoids with frequency $g_c \frac{\sin(\theta_j)}{\lambda}$.
- Use N_c-DFT to estimate θ_j.
- Repeat estimation on various $[n,m]$ to improve the angle estimate.

Pilot Placement in the TF Domain

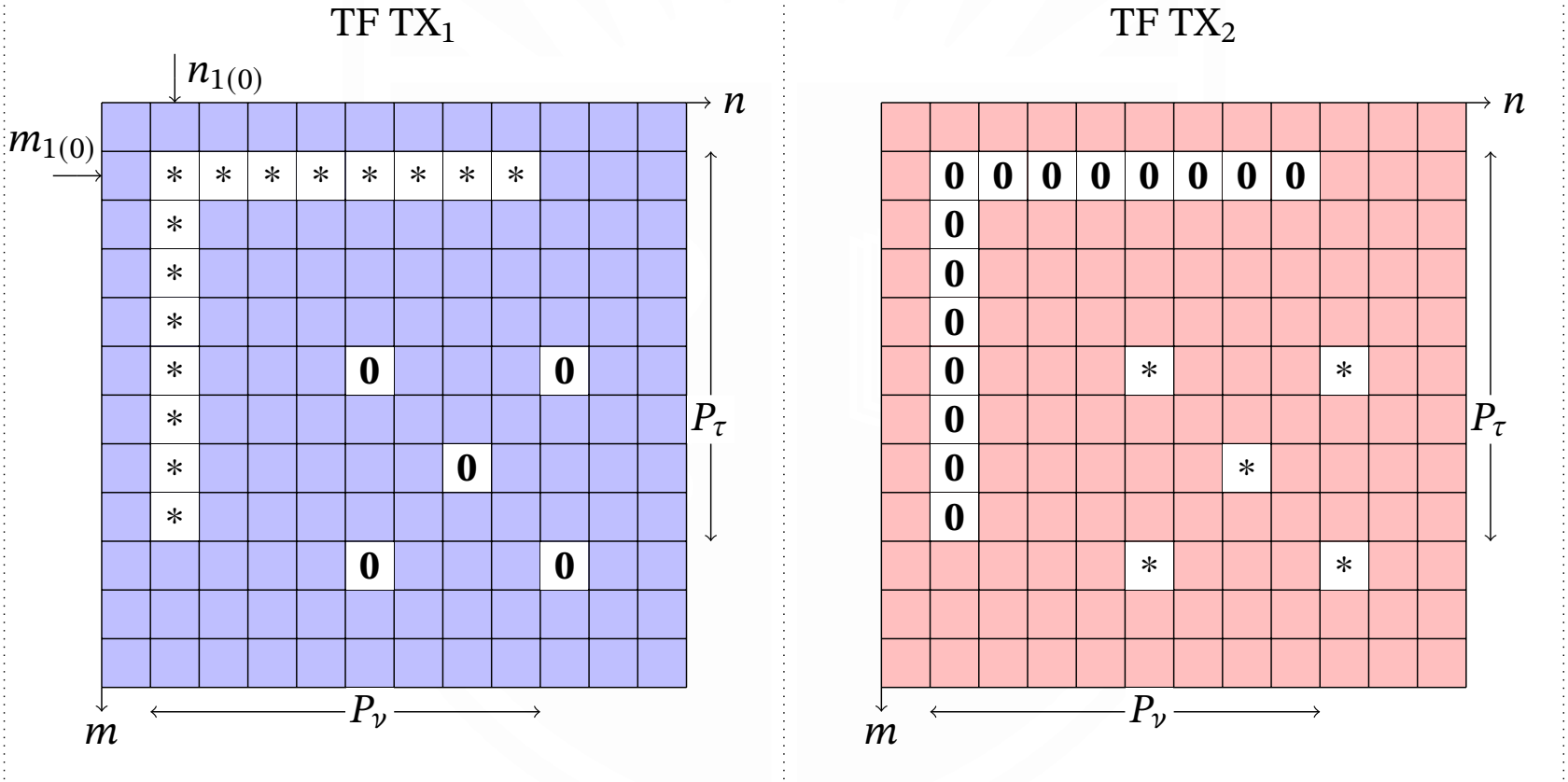

Coarse Estimation of ν_j at the communication receiver

- $\hat{\theta}_j \rightarrow A_j[n,m]$
- Assume N_j scatterers under the same $\hat{\theta}_j$.

$$\frac{A_j[n_p,m_p]}{X_p[n_p,m_p]} = \sum_{j_r=1}^{N_j} e^{-i2\pi p g_t \frac{\sin\phi_{jr}}{\lambda}} H^{j_r}[n_p,m_p],$$

where

$$H^{j_r}[n,m] = \beta_{j_r} e^{-i2\pi \frac{(k_{j_r}+\kappa_{j_r})l_{j_r}}{NM}} e^{i2\pi\left[\frac{(k_{j_r}+\kappa_{j_r})n}{N} - \frac{ml_{j_r}}{M}\right]\xi_{j_r}}.$$

- On the pilot time arm of antenna p we have that

$$\frac{A_j[n_p,m_p]}{X_p[n_p,m_p]} = \sum_{j_r=1}^{N_j} G_{j_r}^t(p,m_p) e^{i2\pi\left[\frac{(k_{j_r}+\kappa_{j_r})n_p}{N}\right]}, \quad n_p = n_{p_0},\ldots,n_{p_0}+P_\nu-1$$

- This is a segment of sum of sinusoids whose frequencies depend on $k_{j_r}+\kappa_{j_r}$ for $j_r = 1,\ldots,N_j$. $\longrightarrow$ Estimate frequencies using a DFT.

Coarse Estimation of τ_j at the Communication Receiver

- Similarly, on the pilot frequency arm of antennas p we have that

$$\frac{A_j[n_p, m_p]}{X_p[n_p, m_p]} = \sum_{j_r=0}^{N_j} G_{j_r}^f(p, n_p) e^{-i2\pi\left[\frac{l_{j_r} m_p}{N}\right]}, \quad m_p = m_{p_0}, \ldots, m_{p_0} + P_\tau - 1$$

- Viewed as function of m_p, this is a segment of sum of sinusoids whose frequencies are related to l_{j_r} for $j_r = 1, \ldots, N_j$. $\longrightarrow$ We can find those frequencies using a DFT.

Coarse Estimation of Angle of Departure (AoD) ϕ_j

Based on estimated θ_j, $R_j = c\tau_j$, and assuming known R_{LoS}, ϕ_j can be obtained by using the law of cosines twice, *i.e.*,

$$(\hat{R}_j - \hat{R}_{cj})^2 = \hat{R}_{jt}^2 = R_{\text{LoS}}^2 + \hat{R}_{cj}^2 - 2R_{\text{LoS}}\hat{R}_{cj}\cos(\hat{\theta}_j) \quad \Rightarrow \hat{R}_{cj} = \frac{\hat{R}_j^2 - R_{\text{LoS}}^2}{2(\hat{R}_j - R_{\text{LoS}}\cos(\hat{\theta}_j))}.$$

$$\hat{R}_{cj}^2 = R_{\text{LoS}}^2 + \hat{R}_{jt}^2 - 2R_{\text{LoS}}\hat{R}_{jt}\cos(\hat{\phi}_j) \quad \Rightarrow \hat{\phi}_j = \arccos\frac{R_{\text{LoS}}^2 + \hat{R}_{jt}^2 - \hat{R}_{cj}^2}{2R_{\text{LoS}}\hat{R}_{jt}}.$$

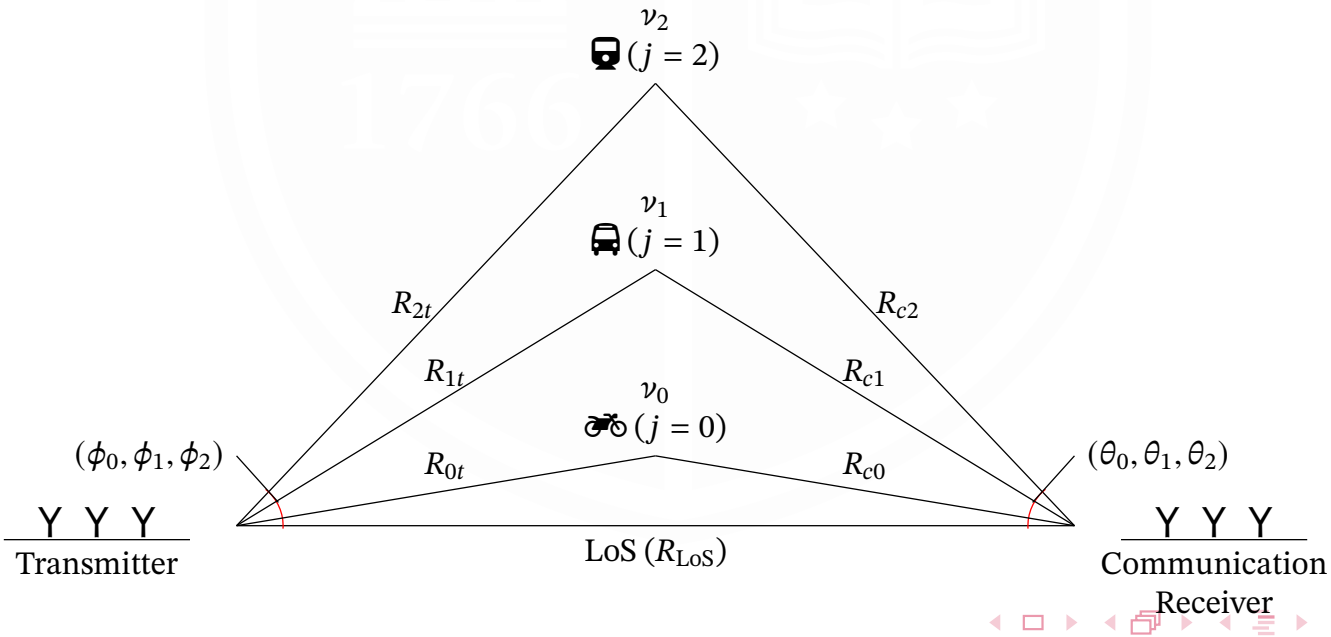

Virtual Array and Sparse Signal Recovery (SSR)

- Place $\frac{Y_{nc}[n_p,m_p]}{X_p[n_p,m_p]}$ of all receive antennas in $\boldsymbol{r}_p$,

$$\boldsymbol{r}_p = \sum_{j=0}^{J-1} \beta_j \boldsymbol{\Phi}_p(\theta_j, \phi_j, \nu_j, \tau_j; n_p, m_p) = \boldsymbol{\Phi}_p \boldsymbol{\beta}.$$

- The (n_c, j)-th element of $\boldsymbol{\Phi}_p$ is

$$e^{-i2\pi n_c g_c \frac{\sin(\theta_j)}{\lambda}} e^{-i2\pi p g_t \frac{\sin(\phi_j)}{\lambda}} e^{-i2\pi \frac{(k_j+\kappa_j)l_j}{NM}} e^{i2\pi\left(\frac{(k_j+\kappa_j)n}{N} - \frac{ml_j}{M}\right)\xi_j}.$$

- Stack all the vectors $\boldsymbol{r}_p$ corresponding to all pilots in vector $\boldsymbol{r} \in \mathbb{C}^{N_p N_c}$:

$$\boldsymbol{r} = \boldsymbol{\Phi}\boldsymbol{\beta}. \quad \text{(virtual array)}$$

- Express $\boldsymbol{r}$ in terms of an overcomplete basis $\tilde{\boldsymbol{\Phi}}$, constructed based on a discretization of the target space around the coarse estimates$(\theta_j, \phi_j, \nu_j, \tau_j)$.
- $\tilde{\boldsymbol{\beta}}$ is a sparse vector, indicating the presence of a target on grid points, which can be obtained by sparse signal recovery (SSR) methods.

Overhead Analysis

- A total number of N_p TF domain pilots requires $N_p(N_t - 1)$ TF domain guard bins and $N_t N_p$ DD domain guard bins.
- The corresponding reduction of DD domain symbols represents an overall overhead of

$$\eta = N_t N_p/(N_t NM) = N_p/(NM).$$

- Overhead independent of the number of transmit antennas $\rightarrow$ good scalability for large MIMO arrays.

Communication with Private Pilots

- After obtaining the refined CSI, to detect the data symbols, we first subtract the pilot contribution from the received signal, *i.e.*,

$$\boldsymbol{y}_{\text{MIMO, data}} = \boldsymbol{y}_{\text{MIMO}} - \hat{\boldsymbol{h}}_{\text{MIMO}} \boldsymbol{x}_{\text{MIMO, pilot}}, \tag{1}$$

  where $\boldsymbol{x}_{\text{MIMO, pilot}}$ is the SFFT of TF pilots, $\boldsymbol{X}_{\text{MIMO, pilot}}$.
- DD guard bins guarantee sufficient linear equations for the LMMSE equalization to recover the transmitted symbols:

$$\hat{\boldsymbol{x}}_{\text{MIMO, data}} = (\hat{\boldsymbol{h}}_{\text{MIMO}}^{\mathsf{H}} \hat{\boldsymbol{h}}_{\text{MIMO}} + N_0 \boldsymbol{I})^{-1} \hat{\boldsymbol{h}}_{\text{MIMO}}^{\mathsf{H}} \boldsymbol{y}_{\text{MIMO, data}}.$$

- $\hat{\boldsymbol{h}}_{\text{MIMO}}$ is highly sparse so that can be solved efficiently by the least-squares with QR factorization (LSQR).
- Finally, $\hat{\boldsymbol{x}}_{\text{MIMO, data}}$ sets DD guard bins positions to zero, completing symbol detection.

System Setup

Table: System Parameters (5G NR FR1)

Symbol	Parameter	Value
f_c	Carrier frequency	4GHz
Δf	Subcarrier spacing	40KHz
M	# of subcarriers	512
N	# of subsymbols	128
$R_{\text{res}} = c\Delta\tau$	Range resolution	7.32m
$v_{\text{res}} = \lambda\Delta\nu$	Speed resolution	11.71m/s

Channel Setup and Coarse Estimation Performance

Table: Example of Scatterers Parameters

j	Coordinates	θ_j°	ϕ_j°	$l_j = l_{cj} + l_{jt}$	$k_j + \kappa_j$
1	$(50.0, -30.5)$	-31.4	-31.4	$8 = 4 + 4$	$-4 - 0.2$
2	$(59.6, 42.4)$	46.4	35.4	$9 = 4 + 5$	$5 + 0.4$
3	$(50.0, -53.5)$	-46.9	-46.9	$10 = 5 + 5$	$4 + 0.1$
4	$(72.5, 10.0)$	20.1	7.9	$7 = 2 + 5$	$-3 - 0.3$

Table: Coarse Estimation Performance

$P_\tau = P_\nu$	SNR = 5dB	Scatter 1		Scatter 2		Scatter 3		Scatter 4	
		mean	std.	mean	std.	mean	std	mean	std
32	θ_j	-32.02	0.39	46	0	-46.05	1.61	19.63	4.62
	l_j	8.01	0.14	9.03	0.19	10.00	0.18	7.04	0.22
	$k_j + \kappa_j$	-4.21	0.05	5.40	0.02	4.06	0.62	-3.31	0.10
64	θ_j	-32.03	0.37	46	0	-46.06	1.62	19.63	4.62
	l_j	8.00	0.00	9.00	0.00	9.99	0.15	7.01	0.10
	$k_j + \kappa_j$	-4.2	0.03	5.40	0	4.05	0.62	-3.31	0.09

NMSE Performance and comparison to the non-overlapped DD pilot approach[15]

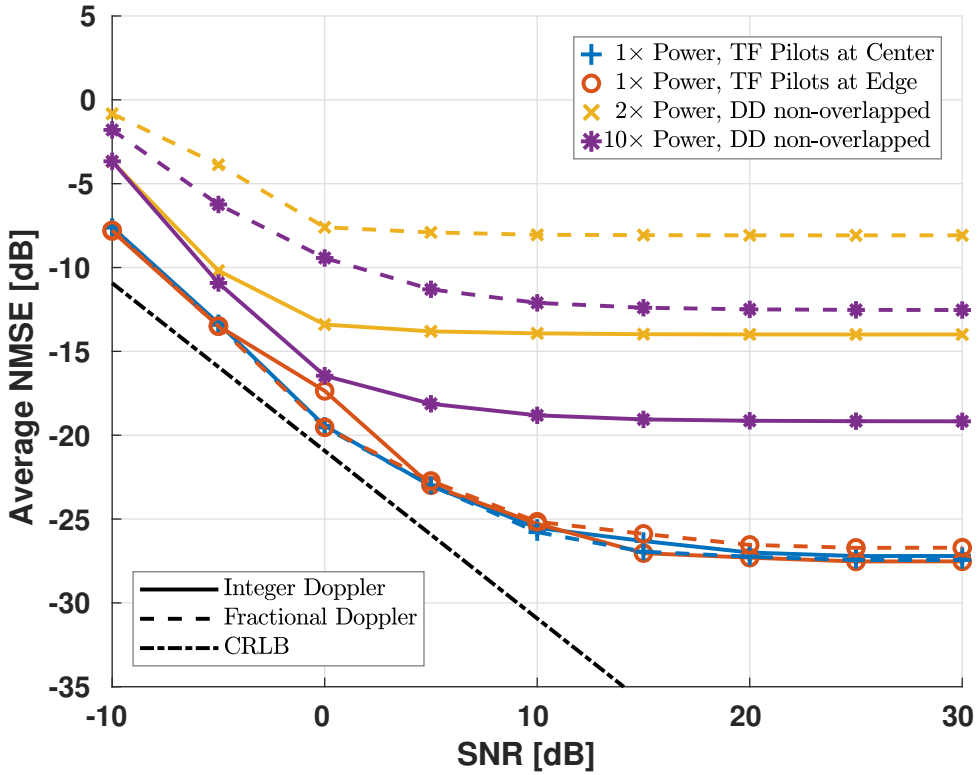

[15] M. Kollengode Ramachandran and A. Chockalingam, "MIMO-OTFS in High-Doppler Fading Channels: Signal Detection and Channel Estimation", in *2018 IEEE Global Communications Conference (GLOBECOM)*, Abu Dhabi, United Arab Emirates: IEEE, Dec. 2018, pp. 206–212, ISBN: 978-1-5386-4727-1. DOI: 10.1109/GLOCOM.2018.8647394.

NMSE Performance for Different Numbers of Pilots

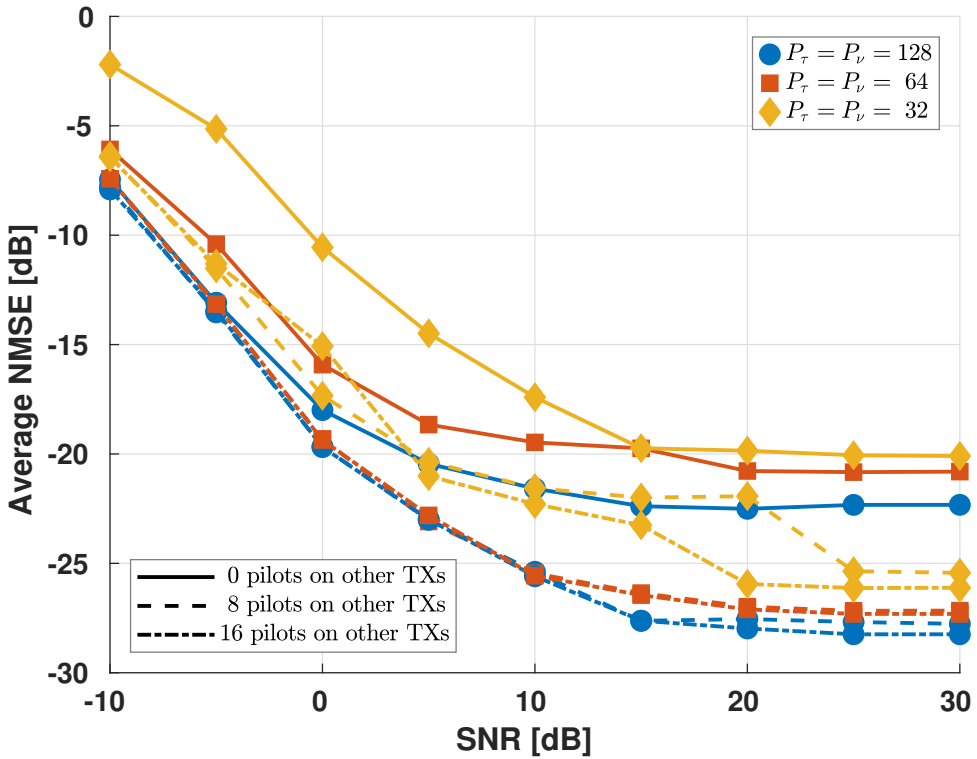

Fig.: NMSE performance of different numbers of pilots.

BER Performance

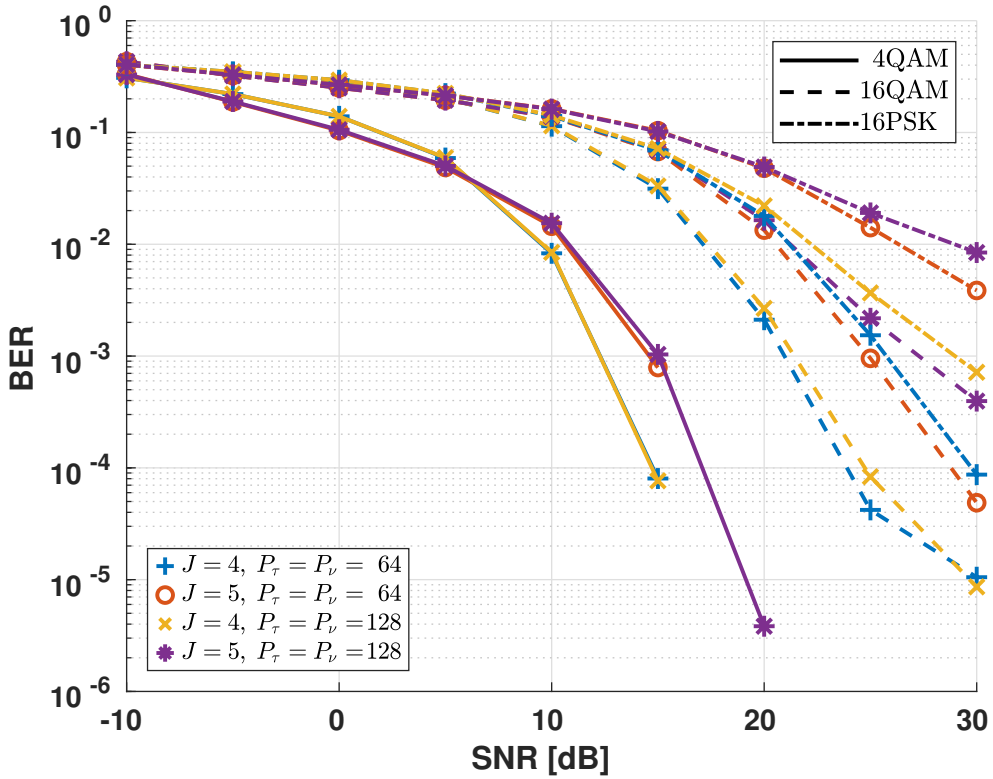

Fig.: BER performance of various modulation, number of scatterers/pilots.

NMSE Performance *vs.* Overlapped DD pilot

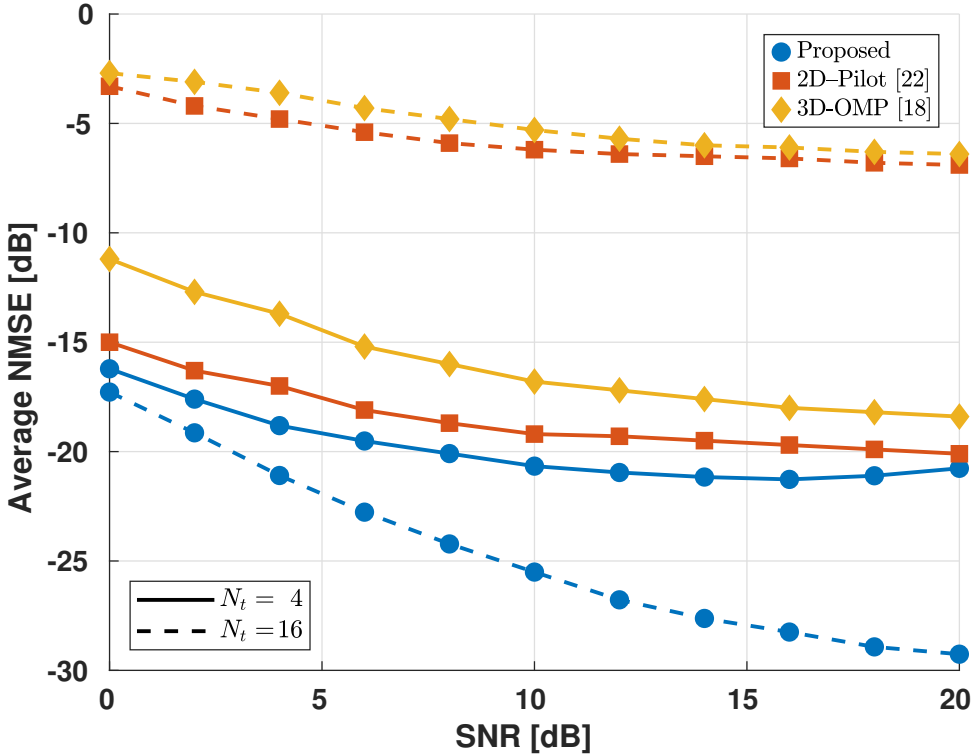

- The overlapped DD pilot designs [6] (3D-OMP), [10] (2D-Pilot) consider downlink transmission from a multi-antenna BS to multiple single-antenna UEs.
- The setup follows [10] ($N_t = \{4, 16\}$, $M \times N = 512 \times 140$, and 121 pilots per TX).

Overhead Comparison

Table: Overhead Comparison ($M = 512, N = 128$)

Pilot Placement	Overhead (η)		$l_{\tau_{\max}} = 10$ $k_{\nu_{\max}} = 6$	$l_{\tau_{\max}} = 15$ $k_{\nu_{\max}} = 10$
Non-overlapped DD pilot [5]	$\frac{[(N_t+1)l_{\tau_{\max}}+N_t][4k_{\nu_{\max}}+1]}{NM}$	$N_t = 4$	2.1%	4.9%
		$N_t = 8$	3.7%	8.9%
Overlapped DD Pilot [6]	$\frac{[2l_{\tau_{\max}}+1][4k_{\nu_{\max}}+1]}{NM}$ (Independent of N_t)		0.8%	1.9%
Proposed TF Pilot	$\frac{N_p}{NM}$ (Independent of N_t)	$P_\tau = P_\nu = 64$	0.02%	0.02%
		$P_\tau = P_\nu = 128$	0.04%	0.04%

Conclusions

- Proposed a Doppler-robust ISAC MIMO-OTFS system that uses shared DD bins for high communication throughput and a small set of private TF bins to form a virtual receive array, enhancing sensing resolution.
- Only a few private bins are sufficient to achieve substantial sensing gains with minimal communication-rate loss.
- Introduced a pilot-placement strategy that enables accurate channel estimation with significantly lower overhead compared to existing MIMO-OTFS methods.

  Open problems: optimal DD guard bin and pilot bin placement
- The required overhead is independent of the number of transmit antennas, providing excellent scalability for large MIMO systems.
- The proposed channel-estimation method is compatible with practical OTFS systems, accounting for rectangular pulse shaping and fractional-Doppler channels.

Reference I

[1] R. Hadani, S. Rakib, M. Tsatsanis, *et al.*, "Orthogonal Time Frequency Space Modulation", in *2017 IEEE Wireless Communications and Networking Conference (WCNC)*, San Francisco, CA, USA: IEEE, Mar. 2017, pp. 1–6, ISBN: 978-1-5090-4183-1. DOI: 10.1109/WCNC.2017.7925924.

[2] M. F. Keskin, C. Marcus, O. Eriksson, A. Alvarado, J. Widmer, and H. Wymeersch, "Integrated Sensing and Communications With MIMO-OTFS: ISI/ICI Exploitation and Delay-Doppler Multiplexing", *IEEE Transactions on Wireless Communications*, vol. 23, no. 8, pp. 10 229–10 246, Aug. 2024, ISSN: 1536-1276, 1558-2248. DOI: 10.1109/TWC.2024.3370501.

[3] K. Wang and A. Petropulu, "ISAC MIMO Systems with OTFS Waveforms and Virtual Arrays", *IEEE Journal on Selected Areas in Communications*, pp. 1–1, 2025, ISSN: 1558-0008, 0733-8716. DOI: 10.1109/JSAC.2025.3608761.

Reference II

[4] K. Wang and A. Petropulu, *Low overhead and scalable time-frequency pilots design for mimo otfs channel estimation*, 2026. arXiv: 2511.08504 [eess.SP]. [Online]. Available: https://arxiv.org/abs/2511.08504.

[5] M. Kollengode Ramachandran and A. Chockalingam, "MIMO-OTFS in High-Doppler Fading Channels: Signal Detection and Channel Estimation", in *2018 IEEE Global Communications Conference (GLOBECOM)*, Abu Dhabi, United Arab Emirates: IEEE, Dec. 2018, pp. 206–212, ISBN: 978-1-5386-4727-1. DOI: 10.1109/GLOCOM.2018.8647394.

[6] W. Shen, L. Dai, J. An, P. Fan, and R. W. Heath, "Channel Estimation for Orthogonal Time Frequency Space (OTFS) Massive MIMO", *IEEE Transactions on Signal Processing*, vol. 67, no. 16, pp. 4204–4217, Aug. 2019, ISSN: 1053-587X, 1941-0476. DOI: 10.1109/TSP.2019.2919411.

Reference III

[7] A. Mehrotra, S. Srivastava, A. K. Jagannatham, and L. Hanzo, "Data-aided csi estimation using affine-precoded superimposed pilots in orthogonal time frequency space modulated mimo systems", *IEEE Transactions on Communications*, vol. 71, no. 8, pp. 4482–4498, 2023. DOI: 10.1109/TCOMM.2023.3280550.

[8] A. Mehrotra, S. Srivastava, S. Asifa, A. K. Jagannatham, and L. Hanzo, "Online Bayesian Learning-Aided Sparse CSI Estimation in OTFS Modulated MIMO Systems for Ultra-High-Doppler Scenarios", *IEEE Transactions on Communications*, vol. 72, no. 4, pp. 2182–2200, Apr. 2024, ISSN: 0090-6778, 1558-0857. DOI: 10.1109/TCOMM.2023.3342230.

[9] K. Wang and A. Petropulu, "Low Overhead MIMO-OTFS Channel Estimation", Accepted by The 33rd European Signal Processing Conference (EUSIPCO 2025).

Reference IV

[10] Y. Liang, P. Fan, Q. Wang, and X. He, "Two-Dimensional Delay-Doppler Pilots and Channel Estimation for Multi-Antenna OTFS in Doubly Dispersive Channels", *IEEE Transactions on Wireless Communications*, vol. 23, no. 7, pp. 7612–7623, Jul. 2024, ISSN: 1536-1276, 1558-2248. DOI: 10.1109/TWC.2023.3342877.